J Therm Anal Calorim (2010) 102:609–613
DOI 10.1007/s10973-010-0915-5

Reaction kinetics of nanometric aluminum and iodine pentoxide

Cory Farley · Michelle Pantoya

NATAS2009 Special Issue

Abstract Owing to increasing threats of biological attacks, new methods for the neutralization of spore-forming bacteria are currently being examined. Thermites may be an effective method to produce high-temperature reactions, and some compositions such as aluminum (Al) and iodine pentoxide (I_2O_5) also have biocidal properties. This study examines the thermal degradation behavior of I_2O_5 mixed with micron and nanometer scale aluminum (Al) particles. Differential scanning calorimetry (DSC) and thermogravimetric (TG) analyses were performed in an argon environment on both particle scales revealing a non-reaction for micron Al and a complex multistep reaction for the nanometer scale Al. Results show that upon I_2O_5 decomposition, iodine ion sorption into the alumina shell passivating Al particles is the rate-controlling step of the Al–I_2O_5 reaction. This pre-ignition reaction is unique to nano-Al mixtures and attributed to the significantly higher specific surface area of the nanometric Al particles which provide increased sites for I^- sorption. A similar pre-ignition reaction had previously been observed with fluoride ions and the alumina shell passivating Al particles.

Keywords Biocidal Reactions · Halogen decomposition · Aluminum combustion · Thermite decomposition

Introduction

The increase of organized terrorist cells around the world poses a growing threat to the United States and many other countries. For these terrorist cells, chemical and biological weapons make highly effective terror weapons against civilians and weapons of intimidation against soldiers [1]. While large scale chemical weapon production requires a large chemical plant, biological weapons can be produced in basements and hospitals around the world [1]. Of the organisms that could cause enough disease and death to cripple a region, anthrax poses one of the greatest threats [2]. Bioweapon attacks from agents such as anthrax would be difficult to predict, detect, or prevent [2]. Therefore, complete elimination of the bacterial spore while in a storage bunker can effectively prevent great loss of life and psychological trauma induced from undergoing a terror attack. Popular methods for the destruction of spore-forming bacteria such as anthrax involve either ultraviolet radiation [3] or an oxidation agent such as peroxide [2]. An assault on a bunker storing anthrax containers does not lend itself to a prolonged ultraviolet radiation exposure. Oxidation of anthrax spores is a slow process with necessary exposure times of up to an hour for effective neutralization [3].

Thermites consist of a mixture of Al and a metal oxide, which produces a highly exothermic reaction when ignited [4]. With flame temperatures over 2000 K, thermites may act as a quick, effective sterilization tool when prolonged exposure to a neutralization agent is not a viable option. A common oxidizer is iron (III) oxide, Fe_2O_3 [5]; however, for bacterial sterilization, I_2O_5 was selected due to iodine's bactericidal properties [6]. Iodine pentoxide is produced by heating iodic acid to 200 °C in a stream of dry air [7]. The remaining powder is stable and produces a thermite reaction when combined with Al fuel. When I_2O_5 and Al react, the products are alumina (Al_2O_3) and iodine, via Eq. 1.

$$10Al + 3I_2O_5 \rightarrow 5Al_2O_3 + 3I_2 \qquad (1)$$

This study examines the kinetics for nanometer and micron scale Al particles reacting with I_2O_5 in a thermal

---

C. Farley · M. Pantoya (✉)
Department of Mechanical Engineering, Texas Tech University, Lubbock, TX 79409-1021, USA
e-mail: michelle.pantoya@ttu.edu; mpantoya@gmail.com

equilibrium experiment from 25 to 1000 °C and in an inert argon (Ar) environment.

Experimental method

Four powder samples were prepared consisting of nanometer scale I_2O_5, 80 nm Al, 15 µm Al, and 40 nm Al_2O_3. The powder characteristics provided by the suppliers are listed in Table 1. Preliminary analysis showed that all the Al is not consumed at the slow heating rates (10 °C min^{-1}) investigated. In order to resolve the reaction kinetics, the Al/I_2O_5 powders were mixed at varying equivalence ratios (ϕ) from 0.4 to 1.2 as is defined by Eq. 2,

$$\phi = \frac{\left(m_f/m_o\right)_{\text{actual}}}{\left(m_f/m_o\right)_{\text{stoichiometric}}} \tag{2}$$

where m_f and m_o are the masses of the fuel and oxidizer, respectively. The Al particles have an Al_2O_3 passivation shell accounting for the material's impurity listed in Table 1. The Al_2O_3/I_2O_5 powder was mixed at a 1:3.27 mass ratio (1:1 molar).

Samples for each of the powders were prepared by suspending the powders in 60 cc of hexane and sonicating the mixture with a Misonix model S3000 for 70 s. In order to prevent damaging the oxide shell passivating the Al particles, the sonicator was programmed to cyclically mix for 10 s, and then to stop, allowing the mixture to cool for 10 s. The solutions were then placed in a glass tray under a fume hood to allow the hexane to evaporate. The powder mixtures were then reclaimed for further experimentation.

The thermal decomposition of each sample was studied with a Netzsch STA 409 differential scanning calorimeter and thermogravimetric analyzer (DSC/TGA). The system was programmed to heat the samples at a rate of 10 °C min^{-1} from room temperature to 1000 °C. Samples of masses of 7 mg were loaded into the sample crucible, and the DSC column was evacuated to less than 0.01 Pa using a Pfeiffer model TMU 071 P turbo molecular drag pump. The column was then backfilled with an argon atmosphere before a 50 mL min^{-1} flow of argon was applied to the furnace for the rest of the heating cycle.

Table 1 Powder characteristics

Material	Particle size	Manufacturer	Purity/%
Al	15 µm	Alfa Aesar	99
Al	80 nm	Nanotechnologies	80
Al_2O_3	40 nm	Nanotechnologies	99.9
I_2O_5		Sigma-Aldrich	99

Results and discussion

The results of the DSC/TG analysis for pure I_2O_5 can be found in Fig. 1. On the left axis, the TG % represents the percent mass change occurring at a given temperature, and on the right, the DSC scale represents the energy change in mW mg^{-1}. Common examples of mass loss are the release of bonded gases, drying of the sample, and a chemical reaction producing gases. Iodine pentoxide bonds with water to become iodic acid, HIO_3 [7]. This reaction becomes reversible and the acid decomposes at 200 °C as shown by

$$3HIO_3 \rightarrow HIO_3 \cdot I_2O_5 \rightarrow 1.5I_2O_5 \tag{3}$$

This decomposition is illustrated in Fig. 1 where the bonded water is released causing the slight mass loss and related endotherm. The I_2O_5 decomposition was observed at an onset temperature of 390 °C where the I_2O_5 fully decomposes into gas corresponding to a 100% mass loss. It is noted that I_2O_5 melting and decomposition are simultaneous [7].

$$I_2O_5 \rightarrow I_2 + 2.5\ O_2 \tag{4}$$

The I_2O_5/Al_2O_3 reaction is displayed in Fig. 2. By combining I_2O_5 and Al_2O_3, the kinetics between I_2O_5 and the Al_2O_3 shell encapsulating the Al particles were isolated. The main differences between Figs. 1 and 2 are the presence of an inflection in the mass loss curve and the presence of a third endotherm with an onset temperature of 460 °C. The inflection point in the mass loss (Fig. 2) may correspond to a slight exothermic behavior causing the heat flow curve to return to the baseline slightly faster than in Fig. 1. The inflection and exotherm may be described by Al_2O_3 binding to either the I_2 or O_2 gas when these oxides disassociate. Since Al_2O_3 is inert to oxygen at this temperature, the reaction must be due to the Al_2O_3 binding to the iodine when freed from disassociating I_2O_5. This is an interesting observation and similar to a study by Osborne and Pantoya [8] that showed fluoride ions from Teflon decomposition bond to the alumina shell passivating Al particles. Sarbak [9] showed the interaction between fluoride ions and Al_2O_3 may be facilitated by hydroxyls that are bonded to a portion of the Al_2O_3 surface. Both of these studies showed that the fluoride ion sorption into alumina was an exothermic reaction [8, 9]. Toyohara et al. [10] studied the iodine sorption mechanism into mixed solid alumina cement. They similarly found that iodine ions replaced hydroxyls and bonded to alumina. Fluorine and iodine are halogens, and this study (as well as others [8–10]) suggests both have similar sorption behaviors when interacting with alumina.

At 550 °C, mass loss in Fig. 2 continues again accompanied by a third endotherm. This second stage of mass

Fig. 1 Heat flow and mass loss curves of I_2O_5, experiments performed in an Ar environment at a heating rate of 10 °C min^{-1}

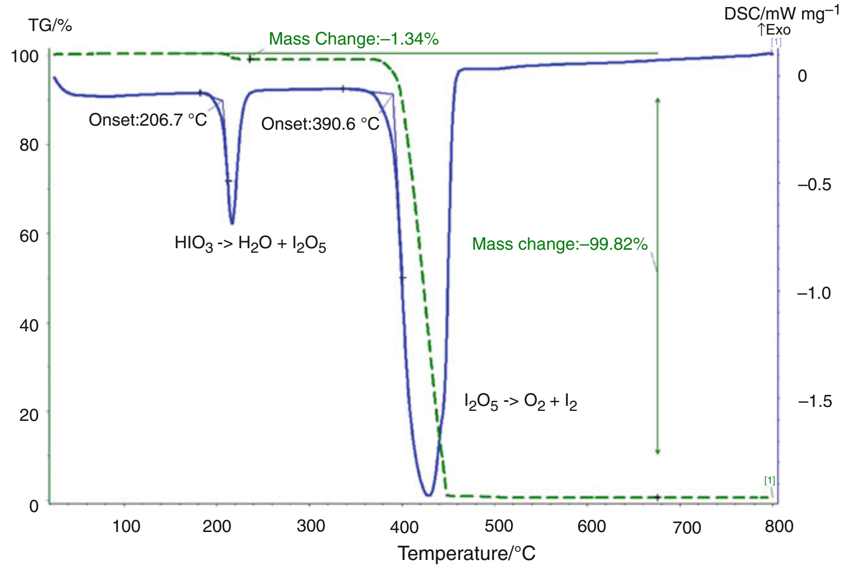

Fig. 2 Heat flow and mass loss curves for Al_2O_3 and I_2O_5, experiments performed in an Ar environment at a heating rate of 10 °C min^{-1}

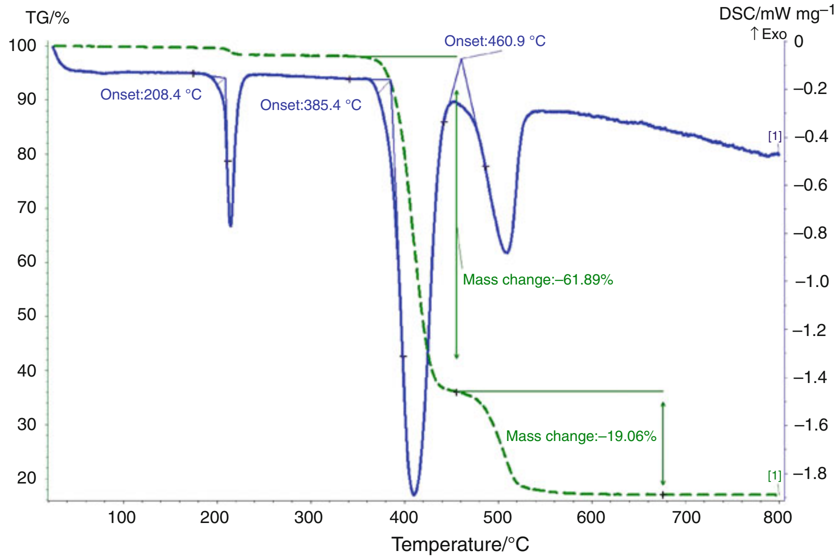

loss and related endotherm may correspond to Al_2O_3 phase changes from amorphous Al_2O_3 to γ-Al_2O_3 [11]. The alumina phase change may trigger a release of iodine gas resulting in a subsequent mass loss.

Figure 3 shows the analysis of the reaction between micron scale Al and I_2O_5. Passivated micron Al has been shown to be thermally nonreactive until it approached its melting temperature of 660 °C [12]. Also, the lower specific surface area of the larger particles reduces the Al_2O_3 shell/I_2O_5 contact area limiting the sorption of iodine into the amorphous Al_2O_3. This specific surface area affect was also observed for the sorption of fluoride ions on varying the specific surface area of Al particles [13]. A combination of the lower specific surface area of the Al particles coupled with the 400 °C degradation of I_2O_5 and the slow heating rate gives the argon gas flowing through the cylinder 22 min to purge the oxygen and iodine gases from the system resulting in the lack of any reaction.

Nanometer scale Al, however, has been shown to be reactive in its solid state at much lower temperatures [8, 12]. This increased reactivity allows the Al to react with the decomposed I_2O_5 as shown in Fig. 4 resulting in a complex multistep process. Similar to Fig. 1, an endotherm appears at 200 °C resulting from iodic acid releasing water and forming I_2O_5. Also, the endotherm at 400 °C corresponding to the decomposition of I_2O_5 can be observed but

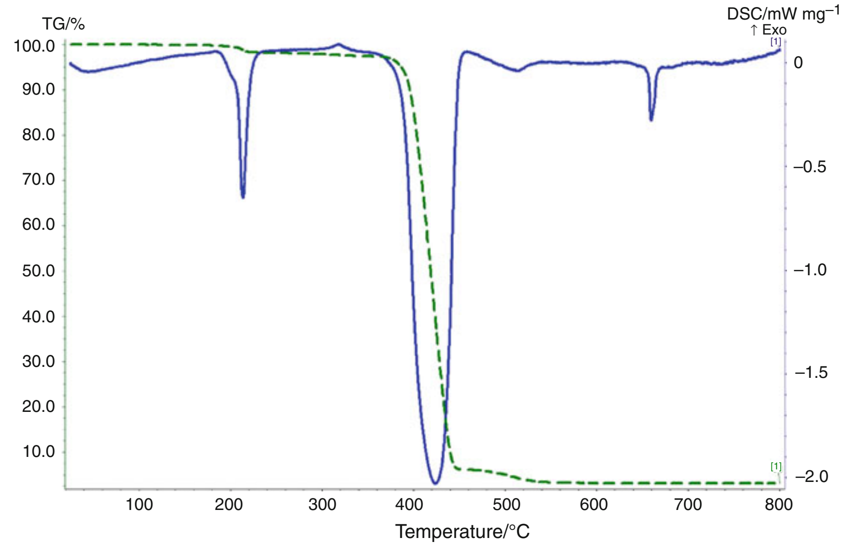

Fig. 3 Heat flow and mass loss curves for micron scale Al and I_2O_5, experiments performed in an Ar environment at a heating rate of 10 °C min^{-1}. Note the lack of any exothermic reaction

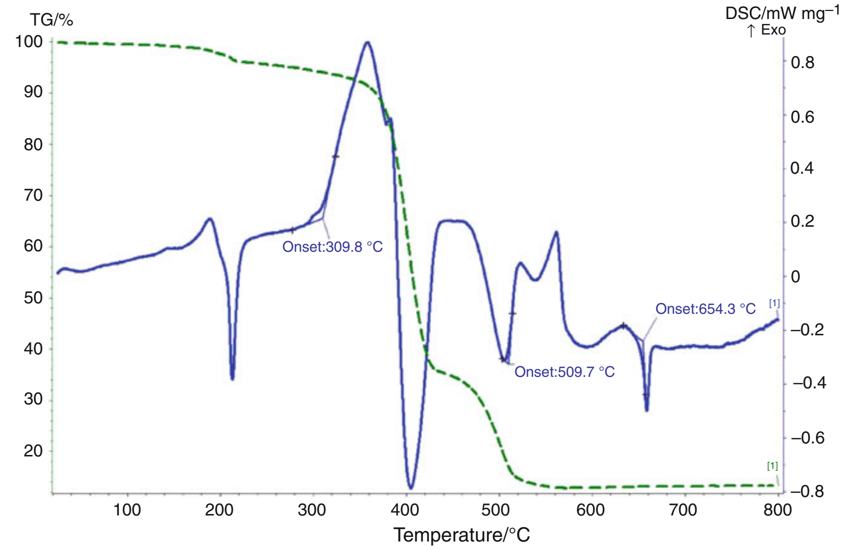

Fig. 4 Nanometer scale Al powder and I_2O_5 with an equivalence ratio of 0.4, experiments performed in an Ar environment at a heating rate of 10 °C min^{-1}

is somewhat masked by the exothermic reaction of Al and oxygen with an onset temperature of 309 °C shown in Eq. 5.

$$4Al + 3O_2 \rightarrow 2Al_2O_3 \quad (5)$$

Examination of the TG curve reveals a similar region to Fig. 2 over 400–550 °C implying an interaction between the Al_2O_3 passivation shell and the iodine gas. Examination of the DSC curve over this temperature range reveals that the endotherm for the iodine release at 400 °C to the alumina phase change at 550 °C is partially masked by an exothermic Al–I–O reaction.

Finally, an endotherm can be seen at 660 °C where unreacted Al melts.

Conclusions

Differential scanning calorimetry (DSC) and thermogravimetric (TG) analysis of I_2O_5, I_2O_5/Al, and I_2O_5/Al_2O_3 mixtures in argon show a scale-dependent reaction based on the size of the Al powder. While larger scale micron powders show little to no reactivity, nanometer scale-passivated Al powders undergo a complex multistep reaction when mixed with I_2O_5. The reaction commences upon I_2O_5 decomposition and is triggered by I^- sorption into the Al_2O_3 passivation shell, further reactions between the iodine and oxygen gas and Al in the solid phase are then observed.

Acknowledgements The authors gratefully acknowledge the support from the Defense Threat Reduction Agency (DTRA) on this project, and the interest and encouragement from our program manager, Dr. Suhithi Peiris.

References

1. Harigel GG. History of biological, chemical, and radiation emergencies. Conference on Biosecurity and Bioterrorism, 2000. p. 1–18.
2. Inglesby TV, Henderson DA, Bartlett JG, Ascher MS, Eitzen E, Friedlander AM, Hauer J, McDade J, Osterholm MT, O'Toole T, Parker G, Perl TM, Russell PK, Tonat K. Anthrax as a biological weapon. J Am Med Assoc. 1999;281:1736–45.
3. Blatchley ER, Meeusen A, Aronson AI, Brewster L. Inactivation of Bacillus spores by ultraviolet or gamma radiation. J Environ Eng. 2005;131(9):1245.
4. Babaitsev IV, Arzhevitov SY, Presnakova OA. Evaluating blast pressure of iron-aluminum thermites. Metallurgist. 2007;51(7–8): 348–350.
5. Dvoryankin AV, Strunina AG, Merzhanov AG. Trends in the spin combustion of thermites. Combust Explos Shock Waves. 1982; 18(2):75–79.
6. Taylor SL, Fina LR, Lambert JL. New water disinfectant: an insoluble quaternary ammonium resin-triiodide combination that releases bactericide on demand. Appl Environ Microbiol. 1970;20(5):720–2.
7. Wiberg E, Wiberg N, Holleman AF, editors. Inorganic chemistry. 1st ed. 2001, p. 465.
8. Osborne DT, Pantoya ML. Effect of particle size on the thermal degradation of Al/teflon mixtures. Combust Sci Technol. 2007;179(8):1467–80.
9. Sarbak Z. Effect of fluoride and sodium ions on structural and thermal properties of gamma-Al_2O_3. Cryst Res Technol. 1997; 32(4):491–7.
10. Toyohara M, Kaneko M, Mitsutsuka N, Fujihara H, Saito N, Murase T. Contribution to understanding iodine sorption mechanism onto mixed solid alumina cement and calcium compounds. J Nucl Sci Technol. 2002;39(9):950–6.
11. Trunov MA, Schoenitz M, Xiaoying Z, Dreizin EL. Effect of polymorphic phase transformations in Al_2O_3 film on oxidation kinetics of aluminum powders. Combust Flame. 2005;140:310–8.
12. Granier JJ, Pantoya ML. Laser ignition of nanocomposite thermites. Combust Flame. 2004;138(4):373–83.
13. Dean SW, Pantoya ML. The influence of alumina passivation on nano-Al/Teflon reactions. Thermochimica Acta. 2009;493(1–2): 109–10.